Hysteresis effect on backwashing process in a submerged hollow fiber membrane bioreactor (MBR) applied to membrane fouling mitigation

Zhao Cui[a], Huu Hao Ngo[b], Zhiyang Cheng[cd], Hongwei Zhang[a], Wenshan Guo[b], Xia Meng[d], Hui, Jia[a], Jie Wang[ad]*

[a] School of Environmental Science and Engineering, State Key Laboratory of Separation Membranes and Membrane Processes, Tianjin Polytechnic University, Tianjin, 300387, China

[b] School of Civil and Environmental Engineering, University of Technology Sydney, Australia

[c] School of Materials Science and Engineering, State Key Laboratory of Separation Membranes and Membrane Processes, Tianjin Polytechnic University, Tianjin, 300387, China

[d] Key Laboratory of Pulp and Paper Science & Technology of Ministry of Education/Shandong Province, Qilu University of Technology (Shandong Academy of Sciences), Jinan, 250353

* Corresponding author:

1. email: wangjiemailbox@163.com (Jie Wang)

Tel.: +86 022 8395 5668;

Abstract

Hysteresis effect on backwashing in a submerged MBR was investigated with dead-end hollow fiber membranes. The out-of-step changes in TMP and flux is the real hysteresis effect which is common but easily overlooked. Methods of visualization and ultrasonic spectrum analysis were implemented. The results showed that fouling layer is just the culprit of hysteresis effect. Fouling level and fiber length were determined as two key factors that affect hysteresis effect by data and model derivation. Moreover, a hysteresis evaluation index "τ_{bw}" is proposed to quantify the result of TMP vs time. The relationship between influence factors and "τ_{bw}" is interactive. A linear relationship between fouling level and "τ_{bw}" was found as well as an extreme value between fiber length and "τ_{bw}". A lower fouling level (lower backwashing flow) and optimal backwashing duration will be helpful for an effective backwashing no matter for membrane fouling control or energy cost reduce.

Keywords: Hysteresis effect; Backwashing; Submerged MBR; Hollow fiber membrane; Hysteresis evaluation index

1. Introduction

A membrane bioreactor (MBR), combining membrane module and bioreactor, has been widely used for municipal and industrial wastewater treatment (Lee et al., 2012) due to its small footprint, better effluent quality, high fouling load capacity, and low sludge production (Nawaz et al., 2019; Vergine et al., 2018; Zheng et al., 2018). However, the serious membrane fouling limits its further application which can lead to: firstly, a dramatic drop in the permeate flux (Cui et al., 2018a; Yang et al., 2019); and secondly, a significant increase in the consumed operational energy (Gao et al., 2018; Lee et al., 2012).

To mitigate membrane fouling, many strategies have been conducted such as membrane cleaning (Hacıfazlıoğlu et al., 2019; Jo et al., 2019), membrane surface modification (Ahmad et al., 2018; Barclay et al., 2018), pretreatment (Wang et al., 2019)and reactor optimization (Vergine et al., 2018; Zheng et al., 2018). Backwashing as an effective method in MBR fouling control has been found to successfully remove fouling deposits and is particularly convenient as a part of a dead-end hollow fiber filtration cycle (Cui et al., 2018a; Jiang et al., 2019). Previous studies of MBR backwashing mainly focused on the optimal backwash frequency, intensity and duration (Hwang et al., 2009; Yigit et al., 2009), and in addition air sparging is used to improve backwash efficiency (Remize et al., 2010). Research into backwashing of recent years has focused on how to maximize the recovery of membrane flux using small amounts of power and short duration conditions (Cogan et al., 2016; Shekhar et al., 2017). Apart from this, novel experimental methods have been conducted with backwashing. Chang et al. (Chang et al., 2016) compared various types of backwash water, including UF permeate, ultrapure water, NaCl solution, $CaCl_2$ solution and sodium alginate solution. Results indicated that UF permeate backwash or $CaCl_2$ solution backwash significantly curtailed the hydraulic cleaning efficiency (HCE). Backwashing with ultrapure water or organic compounds proved to be efficient when both Na^+ and Ca^{2+} were present in feed water. Vera (Vera et al., 2014) assayed an alternative backwashing strategy to enhance water productivity in a tertiary submerged membrane module. After four months of continuous operation, analysis of the membrane fouling showed that backwashing efficiency (described in terms of residual fouling resistance) was significantly affected by the selected TMP_{sp} (transmembrane pressure set-point) value.

These strategies all contribute to helping us understand the effect of operating parameters and backwashing agents in improving the membrane backwashing process. But it still experiences some limitations to evaluate backwashing only through backwashing effectiveness. For example, excessive concentration of backwashing solution can affect the performance of the membrane materials (Fu & Zhang, 2019); The introduction of chemicals and other auxiliary processes will greatly increase the energy consumption of membrane cleaning. Thus, fluid behavioral optimization without the addition of cleaning agents and other auxiliary processes will become the mainstream of future component optimization. However, there are not many researches on how to improve and optimize the cleaning effect through its fluid behavior. Cui et al. (Cui et al., 2018b) investigated the backwashing effectiveness affected by selective permeation of backwashing solution along the fiber length in dead-end hollow fiber membrane system with laser bijection sensing (LBS) technology. This study provides a phenomenon-to-mechanism research method from which our research direction clicked into place and ultimately an explanation on the viability of backwashing effectiveness using a dead-end hollow fiber membrane. In previous studies, a sudden increase was observed in the backwashing flux and this was defined as the hysteresis effect (Wang et al., 2014). The duration required to overcome the hysteresis effect will directly affect the flux recovery of the whole membrane module and the equipment's consumption of energy. Therefore, overcoming the hysteresis effect does make sense in short-term backwashing.

The aim of a series of tests in this study is to investigate the hysteresis effect on a pressure driven hollow fiber membrane backwashing process. Methods of visualization and ultrasonic spectrum analysis were implemented to establish an intuitive understanding of the hysteresis effect. Both the membrane resistance and membrane fouling were taken into account when investigating the hysteresis effect. Moreover, a new parameter named hysteresis evaluation index "τ_{bw}" is proposed to quantify the result of TMP vs time. Effects of fouling level and fiber length on hysteresis effect were also investigated to make clear their contributions to hysteresis effect. This study is expected to provide guidance for an efficient backwashing solution which could contribute to fouling control and energy cost reduce.

2 Materials and methods

2.1 Materials

The pilot-scale MBR was completed in May 2017 at a wastewater treatment plant in

Beijing and was operated for over 365 days with a filtration flux of 35 LMH as well as the capacity of 500 m^3/d (Cui et al., 2018a). The MLSS of the sludge is 10000 mg/L. Sludge is removed every day after the installation starts was well as the sludge kept at 35d. A system designed for the pilot-scale operations is used to control the operation of the MBR system. Hollow fiber membranes used in this MBR were made of PVDF (pore size of 0.2 μm) which was supported by membrane frames.

The material of hollow fiber micro-filtration (MF) membrane provided by Tianjin Motimo Membrane Technology Co., Ltd was pristine polyvinylidene fluoride (PVDF). The dimensions of a positive pressure type membranes used in this study were as follows: the inner/outer diameter, 600/1100 μm; and pore size, 0.22 μm. The peristaltic pump (BT100-2 J, Langer, China) was purchased from Baoding Lange Constant Flow Pump Co., Ltd. Pressure transducer was obtained from Shinaide Transducer Co., Ltd. And the data acquisition card (NI USB-6009, CHENGTEC, USA) was offered by National instruments NI Company.

2.2 Experimental apparatus and preparation

As shown in Fig. 1, all the tests were conducted with constant flow operation. Cleaning agents (deionized water) in raw water tank were sucked through with a peristaltic pump to rinse the membrane fiber from inside to outside. The fibers inserted into two needles were installed by fiber fixing device above the organic glass containers. Three 10 MHz ultrasonic transducers (Panametrics V111, Japan) were placed upon the membrane fibers. The transducers were installed in three organic glass panels which were inlaid on organic glass containers and transducers were driven by a pulser-receiver

(Panametrics 5077PR, Japan). The oscilloscope (Siglent SDS1102A, China) was connected to the pulser-receiver, captured and displayed the amplitude changes in the signal data on its front panel. Ultrasonic data were analyzed utilizing wavelet analysis software.

2.3 Feed suspension characteristics

Due to the long-term operation of the MBR equipment, it is impossible to carry out destructive experiments by cutting down membrane fiber from the module. Thus, the severe fouling condition was created artificially. The fouling experiment was carried out with 1 g/L yeast suspension at a temperature of 20.0 ± 1.0 ºC. This feed suspension was selected in order to get various substances by cells break which can provide different types of membrane fouling and severe fouling conditions during filtration experiments (Wang et al., 2014). The particle size was tested (Mastersizer 2000, Malvern, United Kingdom) with the mean diameter of 2.7μm. The yeast suspension was prepared by mixing the yeast particles with deionized water by a mechanical stirrer and ultrasonic crushing under 20KHz for half an hour, so the solution was appropriate for analyzing the performance of the membrane filtration.

2.4 Ultrasonic spectrum analysis

The principle of ultrasonic spectrum analysis is based on the propagation of mechanical waves. The propagation velocity of a mechanical wave is determined by the property of the medium which it passes through. Once the ultrasound passed through different medias, the acoustic impedance will change, leading to a change in the magnitude of the peak (Li et al., 2013). If the accuracy of the device is high enough, the thickness of the medium can be estimated by the time difference it takes for the reflected wave to arrive. In this study, owing to the stacking of the ultrasonic waveforms from the single hollow fiber membrane and detachment of the fouling layer, waveforms obtained with pure water, different concentrations of yeast solution, fouling layer and membrane were considered as the references. (Cui et al., 2017).

3 Results and discussion

3.1 Mechanism of hysteresis effect

In the former study (Wang et al., 2014) , an abrupt change in backwashing TMP (flux) was perceived in the continuous membrane backwashing procedure. It is evident that the TMP (flux) increased sharply in the first minute of backwashing after which the trend slowed down but then increased gradually. Thus, the TMP variation of the first minute was accurately investigated. The phenomenon can be described as no water production at first, but then later on as non-uniform water production in membrane backwashing. This is what we call the hysteresis effect.

To better understand this scenario, a detailed study of hysteresis effect was conducted with the improved setup (Wang et al., 2014) shown in Fig. 1. An intuitive explanation was made that the hysteresis effect can be described as the out-of-step changes in TMP and flux in backwashing process as shown in Fig.2(a). The backwashing process was operated under the flow of 85L/h with 0.6 m membrane. As it can be seen, the TMP increased sharply after which the trend slowed down to a bottom at the moment of 18 s, but then increased gradually. Then looking flux variation, there was no backwashing flux measured in the first 13 s followed by a sharp increase to a peak at 18 s after which the trend slowed and became stable. The lowest TMP inside the fiber lumen was corresponding to the highest flux. The out-of-step changes in TMP and flux was just the real hysteresis effect.

The mechanism of hysteresis effect was assumed to occur in four states as shown in Fig. 2(b). In the first state, a tight cake formed and the cleaning agents did not permeate into the fouling layer. In the second state, the permeation of cleaning agents caused cake layer swelling and TMP increase in fiber lumen. The third state was a porous cake in which the layer swelled to extreme state but do not detach as well as the TMP increased to a maximum value. In the last state, the fouling layer's water storage capacity became saturated and then the layer broke off which resulted in a sharply decrease of TMP.

3.2 The factors that caused the hysteresis effect

3.2.1 Hysteresis effect caused by fouling layer

Since the influencing factors of hysteresis effect are complex, effect of the fouling layer to the hysteresis effect is investigated in this section. State of hysteresis effect using a 0.6 m membrane was observed directly by an interchangeable lens digital microscope (B011, Supereyes, China) under the backwashing flow of 85 L/h with pure water. The reason for choosing this scale it is because it can provide a sufficient amount of backwashing effect and a clearly observed trend in TMP variation. The membrane fibers here were all pre-pressured. Details will be shown in section 3.2.2.

Fig. 3 shows the TMP variation compared to the digital photos. It can be seen that the TMP tended to first slowly increase and this was followed by a sharply increase to a peak, after which the TMP slowed down and gradually became stable. The variation in the fouling layer is illustrated in the digital photos. A thick yeast fouling layer could be seen on the membrane surface at stage (a) when the pump was opened. The fouling layer swelled by absorbing pure water after the backwashing agents permeate through the membrane surface at stage (b). After that the fouling layer continued to absorb pure water to the maximum volume at stage (c). Finally, the fouling layer ruptured and the hysteresis effect ended at stage (d). The results indicated that the fouling layer functions to retain water. The total resistance should contain the fouling layer's resistance and the surface tension of the liquid et al.

In order to improve the results' credibility, a method of ultrasonic spectrum analysis was implemented to monitor the hysteresis effect. The hysteresis effect of the fouling layer with a 0.6 m fouled membrane was measured again with the ultrasonic spectrum under the backwashing flow of 85 L/h with pure water. The data of monitoring point at the end point of membrane (Fig. 1) was chosen to describe the hysteresis effect. The reason for selecting this data was that the pressure of end membrane point was the lowest that corresponded to the slowest hysteresis effect which was thought to be easy to analyze. In Fig. 4, the ultrasonic amplitude variation and 2D contour diagram of the hysteresis effect was depicted. This result indicated that the ultrasonic signal passed through air, fouling layer, membrane top surface, respectively. 2D contour diagram of Fig. 4 (a) made a more intuitive description of the fouled membrane as well as the fouling layer thickness calculated as 85μm. As for Fig. 4 (b), The fouling layer swelled and filled the gap between the ultrasonic probe and the membrane of 153μm. That swelling of fouling layer should attribute to hysteresis effect. Meanwhile, the dilution of the fouling layer resulted in a weakening of the ultrasonic signal. This result indicated that the fouling layer swelled by absorbing backwashing duration and the hysteresis effect did exist in the backwashing process.

3.2.2 Hysteresis effect caused by the membrane

As the fouling layer confirmed to make contribution to hysteresis effect, the effect of membrane was investigated in this section. A virgin membrane fiber was backwashed directly using a 0.6 m membrane under the backwashing flow of 85 L/h with pure water. The TMP variation was similar as that of Fig. 3 which showed a trend of first increase to a peak then dropped off and remained stable. It can attribute to residual substances inside the membrane pores which caused the hysteresis effect on the membrane itself. Thus, the solution for removing residual substances were applied called pre-pressure treatment.

Pre-pressure treatment refers to backwash of virgin membrane fibers which had no fouling. In these tests, the hysteresis effect slowed down when the pre-pressure treatment duration increased. When the pre-pressure duration increased to 15 minutes, the hysteresis effect caused by the membrane disappeared. This phenomenon suggested that the hysteresis effect caused by the membrane can be avoided if a pretreatment strategy is implemented.

3.3 Determination of hysteresis evaluation factor

Transmembrane membrane pressure (TMP) changes vs time was often used in the investigation of membrane process. It can not only test the sealing of device but can evaluate the real-time changes of operation process. But when comparing the TMP variation with others, the problems will appear. If the maximum values of the two curves are different and will not overlap, then it is easy to distinguish the TMP. But if the maximum values of the two curves are the same and the final curves overlap, it will be difficult to give the comparison. Thus, a new index named hysteresis evaluation index "τ_{bw}" is proposed to quantify the result of TMP vs time. Here, "τ_{bw}" represents the area enclosed by TMP curve and X axis. Here, the new hysteresis duration was defined as from the pump open to the time that TMP get stable. The calculation method is shown in Eq. (1):

$$\tau_{bw} = \int_0^t P\, dt \qquad (1)$$

In order to verify the practical significance of "τ_{bw}", the following verification has been made. Energy consumption is an important indicator of actual engineering operation. When mentioned the energy consumption, it is acting as shown in Eq. (2):

$$W = PV \qquad (2)$$

Where W is for power of backwashing (Pa·m^3); P is for backwashing transmembrane pressure inside fiber lumen (Pa); V is for the volume of liquid in the lumen (m^3).

According to flow calculation formula, the Eq. (2) should be rearranged to Eq. (3):

$$W = PV = PQt \qquad (3)$$

Where Q is for backwashing flow (m^3/s); t is for backwashing duration (s).

By combining the Hagen–Poiseuille equation and the hydrostatic equation, pressure drop of backwashing process in the lumen side can be described as Eq. (4) (Wang et al., 2014),

$$\frac{d^2P(x)}{dx^2} - \lambda^2 P(x) = 0 \tag{4}$$

$$\lambda = \sqrt{\frac{128 D_0 \mu k}{{D_i}^4}} \tag{5}$$

where μ is the dynamic viscosity of the backwashing solution; D_i and D_0 are inner and outer diameter of hollow fiber membrane (m); k is for a coefficient of backwashing; One can then obtain Eq. (6):

$$P(x) = c_1 e^{\lambda x} + c_2 e^{-\lambda x} \tag{6}$$

Where c_1 and c_2 are constant.

To further investigate the effect of on flux distribution, a module with fouling was developed (Wang et al., 2014). It assumed a semi-aqueous operational length (L_{sa}) under which the fiber cannot be cleaned. The L_{sa} starts at the dead end of the fiber. The reason can be assessed as that the fouling layer preferentially dropped from the upper part of hollow fiber membrane at the onset of backwashing operating due to a high local flux in this area. TMP under the semi-aqueous operational length also satisfy the differential Eq. (4). The other boundary condition changed to Eq. (7) owing to the increase of the backwashing resistance in the semi-aqueous operational length of the hollow fiber membrane:

$$\int_0^{L_{sa}} J_1(x)dx + \int_{L_{sa}}^{L} J_2(x)dx = LJ_e \tag{7}$$

Then the constant c_1 and c_2 in Eq. (6) can be described as:

$$c_1 = LJ_e / \left\{ k_1 \frac{e^{\lambda_1 L_{sa}} + e^{2\lambda_2 L} - e^{2\lambda_2 L - \lambda_1 L_{sa}} - 1}{\lambda_1} + k_2 \frac{e^{2\lambda_2 L - \lambda_2 L_{sa}} - e^{\lambda_2 L_{sa}}}{\lambda_2} \right\} \tag{8}$$

$$c_2 = c_1 e^{2\lambda_2 L} \tag{9}$$

where subscript 1 and 2 in parameters λ and k are used for semi-aqueous cleaning and normal cleaning regions, respectively.

Based on (6), (8) and (9), the flux distribution can also be described by Eq. (10):

$$J(x) = \begin{cases} k_1(c_1 e^{\lambda_1 x} + c_2 e^{-\lambda_1 x}) & \text{if} \quad 0 \le x < L_{sa} \\ 0 & \text{if} \quad L_{sa} < x < L \end{cases} \tag{10}$$

Where $J(x)$ is local flux of backwashing (L/m^{2}h). Once the unknown variables c_1 and c_2 are calculated by the aforementioned boundary conditions and assumed that the region of length L_{sa} is blocking, the transmembrane pressure distribution along the fiber can be expressed as Eq. (11):

$$P(x) = \begin{cases} \dfrac{LJ_e\lambda(e^{\lambda x} + e^{2\lambda L - \lambda x})\mu R_t}{e^{\lambda(2L - L_{sa})} - e^{\lambda L_{sa}}}, & \text{if} \quad 0 \le x < L_{sa} \\ 0, & \text{if} \quad L_{sa} < x < L \end{cases} \tag{11}$$

Where R_t is the total membrane resistance. According to Eq. (3), the energy consumption of backwashing can be calculated as Eq. (12):

$$W(x) = \begin{cases} P(x) \cdot Qt, & \text{if} \quad 0 \le x < L_{sa} \\ C, & \text{if} \quad L_{sa} < x < L \end{cases} \tag{12}$$

Where Q is the backwashing flow (L/h). If the backwashing process is operated under a constant flow condition, the P(x) will be always changing, thus the energy of backwashing could be calculated as Eq. (13):

$$W(x) = \begin{cases} Q\int_0^t P(x)dt, & \text{if} \quad 0 \le x < L_{sa} \\ C, & \text{if} \quad L_{sa} < x < L \end{cases} \tag{13}$$

By combining Eq. (1) and (13) the energy consumption of backwashing could be shown as Eq. (14):

$$W(x) = \begin{cases} Q\tau_{bw}, & \text{if} \quad 0 \le x < L_{sa} \\ C, & \text{if} \quad L_{sa} < x < L \end{cases} \tag{14}$$

Where C is the maximum value of $Q\tau$. Eq. (14) indicated that energy consumption is proportional to fiber length within the effective backwash length. While, there is a maximum valid value if the fiber length is overlength. Thus, the "τ_{bw}" here as an index of energy equation did have a practical significance which could be used as a quantitative standard in constant flow backwashing. The unit of "τ_{bw}" here is Pa·s;

3.4 Key factors that affect the hysteresis effect

It can be obtained from section 3.2.1 and 3.3 that fouling level and fiber length are two key factors that affect the hysteresis effect. Thus, the effects of the two key factors would be investigated in the following sections.

As the hysteresis effect of the membrane can be avoided by pretreatment, a further investigation should be made on the effect of fouling layer. Thus, an influencing factor of fouling level is imported to make a better understanding of hysteresis effect.

The fouling level is quantified by the transmembrane pressure (TMP). The filtration process was operated under the permeate flux of 100 L/m^{2}h for the single membrane (Cui et al., 2018b). Furthermore, the reversible fouling layer and pore blocking represent the main fouling types.

As the filtration TMP increased to 20 kPa, the filtration process was stopped. This fouling level was defined as FL-20kPa. Similarly, other three fouling levels of FL-30kPa, FL-40kPa and FL-50kPa were chosen to make a comparation. The 50 kPa here was monitored as the critical TMP. After that backwashing process began with the different fouling levels under the backwashing flow of 85 L/h which was measured as the optimal backwashing flow of 0.6 m membrane (Cui et al., 2017; Wang et al., 2014). And the TMP variation and the hysteresis condition were shown in Fig. 5. The hysteresis effect could also be found in the TMP variation Fig. 5(a). As the backwashing began, the TMP of FL-20kPa reached the peak at 7.5 s with the value of 57 kPa then dropped down to a bottom at 12.5 s with the value of 23 kPa. After that the TMP gradually got stable. The TMP difference of peak and bottom was 34 kPa. This result indicated that the shedding of the cake layer at the end of the hysteresis effect resulted in a TMP decrease inside the membrane lumen. Looking at the variation of FL-30kPa, FL-40kPa and FL-50kPa, the trend of TMP variation were similar with each other while the difference was also obvious. With the increase of fouling level, the backwashing duration and "τ_{bw}" were also increased. It indicated that the more serious the fouling, the longer time was required for overcoming the hysteresis effect. In other words, more serious the fouling, the longer time and more energy were required for backwashing. Looking at Fig. 5(b-d), the trend of TMP variations were similar as that of (a). It is noteworthy that once the fouling degree was known, the maximum TMP inside fiber lumen was also determined. With the increase of fiber length, the only difference was that the hysteresis duration extended which resulted in an increase of "τ_{bw}".

As for the effect of fiber length, a series of tests are also conducted. The fouling levels were also divided to FL-20, 30, 40, 50kPa as shown in Fig.5. The only difference was the hysteresis duration. In other words, the value of "τ_{bw}" increased with the increase of fiber length under the same fouling level. The TMP value of the peak and bottom had no change when operated with the same fouling level no matter how long the membrane fiber was. The reason was that the resistance of fouling layer was limited. Thus, the TMP required to overcome the hysteresis effect has a maximum value when the fouling level was determined. The only difference was that the hysteresis duration was extended with the increase of fiber length. The reason was that backwashing solution required more time to arrive at the most distant membrane which leaded to extension of duration that TMP arrived the peak with a higher "τ_{bw}". This result indicated that longer fiber needs more duration to achieve an effective backwashing.

The contributions of fouling level and fiber length to hysteresis effect were not obvious. Thus, more parallel tests were carried out. First, the fouling levels were added as FL-60kPa and FL-70kPa as well as the fiber length were added as 1.8 and 2.1 m. After a series of tests, a conclusion can be made that the hysteresis duration and the value of "τ_{bw}" were always increased with the increase of fouling level even if it was higher than the critical fouling level. But there was an effective backwashing length when backwashing flow was fixed no matter how long the actual fiber was.

A comprehensive evaluation for effect of fouling level and fiber length on hysteresis effect was made by the hysteresis evaluation index as shown in Fig. 6. As the increase of fouling level, the value of hysteresis evaluation index followed the same trend. There is a linear relationship between fouling level and "τ_{bw}". When looking at the effect of fiber length, the "τ_{bw}" increased gradually as the fiber length increased from 0.6 to 1.5 m. But the value can't increase infinitely and there exists a maximum value. When the fiber length increased to 1.8 and 2.1 m, the value of "τ_{bw}" almost stay the same. The relationship between fiber length and "τ_{bw}" was not liner but extreme. Generally, the maximum hysteresis evaluation index can be obtained when fouling level and backwashing flow is fixed no matter how long the fiber is. The experimental results here was just coincide with the theoretical predictions of section 3.3. The membranes with low fouling level require shorter duration to overcome the hysteresis effect. Moreover, longer membranes don't have to deliberately delay the backwashing duration but just need to overcome the resistance of fouling layer. The membranes with low fouling level require shorter duration to overcome the hysteresis effect. Moreover, longer membranes don't have to deliberately delay the backwashing duration but just need to overcome the resistance of fouling layer.

Finally, a conclusion can be obtained that fouling level and fiber length all make contribution to hysteresis effect in the constant flow backwashing within the effective length. Once the backwashing flow can't provide an effective backwashing to the longer fiber, the fouling level will be the decisive factor affecting the hysteresis effect. If an effective backwashing is wanted in engineering applications under constant flow operation, a lower fouling level (lower backwashing flow) and optimal backwashing duration will be helpful.

4 Conclusion

The fouling layer was the main factor that caused the hysteresis effect while the hysteresis effect caused by the membrane could be eliminated via pretreatment during the MBR backwashing process. Hysteresis evaluation index "τ_{bw}" was proposed quantify the result of TMP vs time. There is a linear relationship between fouling level and "τ_{bw}". The relationship between fiber length and "τ_{bw}" was not liner but extreme. A lower fouling level (lower backwashing flow) and optimal backwashing duration will be helpful for an effective backwashing no matter for membrane fouling control or energy cost reduce.

E-supplementary data for this work can be found in e-version of this paper online.

Nomenclature

τ_{bw} hysteresis evaluation index (Pa·s)

P backwashing transmembrane pressure (kPa)

W power of backwashing (Pa·m^3)

F pressure inside fiber lumen (N)

V volume of liquid in the lumen (m^3)

Q backwashing flow (m^3/s)

L fiber length (m)

t backwashing duration (s)

μ dynamic viscosity of the backwashing solution

D_i, D_0 inner and outer diameter of hollow fiber membrane (m);

k a coefficient of backwashing

L_{sa} a semi-aqueous operational length (m)

R_t total membrane resistance(m^{-1})

J(x) local flux of backwashing (L/m^2h).

Acknowledgments

This study was financially supported by the National Natural Science Foundation of China (No.51978464), The Project was also supported by the Foundation (No. KF201919, KF201807) of Key Laboratory of Pulp and Paper Science and Technology of Ministry of Education/Shandong Province of China. The research collaboration between Tianjin Polytechnic University and University of Technology Sydney is grateful.

References

Ahmad, R., Kim, J.K., Kim, J.H., Kim, J. 2018. Effect of polymer template on structure and membrane fouling of TiO2/Al2O3 composite membranes for wastewater treatment. *Journal of Industrial and Engineering Chemistry*, **57**, 55-63.

Barclay, T.G., Hegab, H.M., Michelmore, A., Weeks, M., Ginic-Markovic, M. 2018. Multidentate polyzwitterion attachment to polydopamine modified ultrafiltration membranes for dairy processing: Characterization, performance and durability. *Journal of Industrial and Engineering Chemistry*, **61**, 356-367.

Chang, H., Liang, H., Qu, F., Shao, S., Yu, H., Liu, B., Gao, W., Li, G. 2016. Role of backwash water composition in alleviating ultrafiltration membrane fouling by sodium alginate and the effectiveness of salt backwashing. *Journal of Membrane Science*, **499**, 429-441.

Cogan, N.G., Li, J., Badireddy, A.R., Chellam, S. 2016. Optimal backwashing in dead-end bacterial microfiltration with irreversible attachment mediated by extracellular polymeric substances production. *Journal of Membrane Science*, **520**(Supplement C), 337-344.

Cui, Z., Wang, J., Zhang, H., Jia, H. 2017. Influence of released air on effective backwashing length in dead-end hollow fiber membrane system. *Journal of Membrane Science*, **530**, 132-145.

Cui, Z., Wang, J., Zhang, H., Ngo, H.H., Jia, H., Guo, W., Gao, F., Yang, G., Kang, D. 2018a. Investigation of backwashing effectiveness in membrane bioreactor (MBR) based on different membrane fouling stages. *Bioresource Technology*, **269**, 355-362.

Cui, Z., Wang, J., Zhang, H., Song, L., Jia, H., Yang, G., Gao, F. 2018b. Influence of selective permeation of backwashing solution on the cleaning effectiveness in hollow fiber system. *Journal of Membrane Science*, **546**(Supplement C), 139-150.

Fu, W., Zhang, W. 2019. Chemical aging and impacts on hydrophilic and hydrophobic polyether sulfone (PES) membrane filtration performances. *Polymer Degradation and Stability*, **168**, 108960.

Gao, F., Wang, J., Zhang, H., Jia, H., Cui, Z., Yang, G. 2018. Role of ionic strength on protein fouling during ultrafiltration by synchronized UV–vis spectroscopy and electrochemical impedance spectroscopy. *Journal of Membrane Science*, **563**, 592-601.

Hacıfazlıoğlu, M.C., Parlar, İ., Pek, T.Ö., Kabay, N. 2019. Evaluation of chemical cleaning to control fouling on nanofiltration and reverse osmosis membranes after desalination of MBR effluent. *Desalination*, **466**, 44-51.

Hwang, K.-J., Chan, C.-S., Tung, K.-L. 2009. Effect of backwash on the performance of submerged membrane filtration. *Journal of Membrane Science*, **330**(1), 349-356.

Jiang, C.-K., Tang, X., Tan, H., Feng, F., Xu, Z.-M., Mahmood, Q., Zeng, W., Min, X.-B., Tang, C.-J. 2019. Effect of scrubbing by NaClO backwashing on membrane fouling in anammox MBR. *Science of The Total Environment*, **670**, 149-157.

Jo, Y., Johir, M.A.H., Cho, Y., Naidu, G., Rice, S.A., McDougald, D., Kandasamy, J., Vigneswaran, S., Sun, S. 2019. A comparative study on nitric oxide and hypochlorite as a membrane cleaning agent to minimise biofilm growth in a membrane bioreactor (MBR) process. *Biochemical Engineering Journal*, **148**, 9-15.

Lee, E.-J., Kim, K.-Y., Lee, Y.-S., Nam, J.-W., Lee, Y.-S., Kim, H.-S., Jang, A. 2012. A study on the high-flux MBR system using PTFE flat sheet membranes with chemical backwashing. *Desalination*, **306**, 35-40.

Li, X., Li, J., Wang, J., Wang, H., He, B., Zhang, H. 2013. Ultrasonic visualization of sub-critical flux fouling in the double-end submerged hollow fiber membrane module. *Journal of Membrane Science*, **444**, 394-401.

Nawaz, M.S., Parveen, F., Khan, S.J., Hankins, N.P. 2019. Impact of osmotic backwashing, particle size distribution and feed-side cross-flow velocity on flux in the forward osmosis membrane bioreactor (FO-MBR). *Journal of Water Process Engineering*, **31**, 100861.

Remize, P.J., Guigui, C., Cabassud, C. 2010. Evaluation of backwash efficiency, definition of remaining fouling and characterisation of its contribution in irreversible fouling: Case of drinking water production by air-assisted ultra-filtration. *Journal of Membrane Science*, **355**(1), 104-111.

Shekhar, M., Shriwastav, A., Bose, P., Hameed, S. 2017. Microfiltration of algae: Impact of algal species, backwashing mode and duration of filtration cycle. *Algal Research*, **23**(Supplement C), 104-112.

Vera, L., González, E., Díaz, O., Delgado, S. 2014. Application of a backwashing strategy based on transmembrane pressure set-point in a tertiary submerged membrane bioreactor. *Journal of Membrane Science*, **470**, 504-512.

Vergine, P., Salerno, C., Berardi, G., Pollice, A. 2018. Sludge cake and biofilm formation as valuable tools in wastewater treatment by coupling Integrated Fixed-film Activated Sludge (IFAS) with Self Forming Dynamic Membrane BioReactors (SFD-MBR). *Bioresource Technology*, **268**, 121-127.

Wang, J., Cui, Z., Jia, H., Zhang, H. 2014. The effect of fiber length on non-uniform and hysteresis phenomenon in hollow fiber membrane backflushing. *Desalination*, **337**, 98-108.

Wang, X., Zhu, H., Sun, T., Liu, Y., Han, T., Lu, J., Dai, H., Zhai, L. 2019. Synthesis and Study of an Efficient Metal-Organic Framework Adsorbent (MIL-96(Al)) for Fluoride Removal from Water. *Journal of Nanomaterials*, **2019**, 13.

Yang, G., Wang, J., Zhang, H., Jia, H., Zhang, Y., Gao, F. 2019. Applying bio-electric field of microbial fuel cell-upflow anaerobic sludge blanket reactor catalyzed blast furnace dusting ash for promoting anaerobic digestion. *Water Research*, **149**, 215-224.

Yigit, N.O., Civelekoglu, G., Harman, I., Koseoglu, H., Kitis, M. 2009. Effects of various backwash scenarios on membrane fouling in a membrane bioreactor. *Desalination*, **237**(1), 346-356.

Zheng, Y., Zhang, W., Tang, B., Ding, J., Zheng, Y., Zhang, Z. 2018. Membrane fouling mechanism of biofilm-membrane bioreactor (BF-MBR): Pore blocking model and membrane cleaning. *Bioresource Technology*, **250**, 398-405.

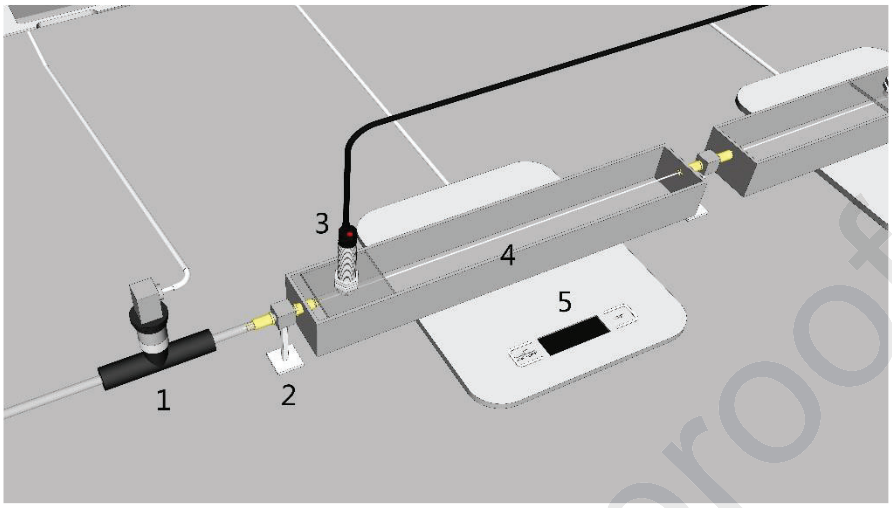

Fig. 1 Membrane filtration & backwashing system:

1, Pressure sensor; 2, Fiber fixing device; 3, Ultrasonic monitoring point 1; 4, Membrane fiber; 5, Electronic balance

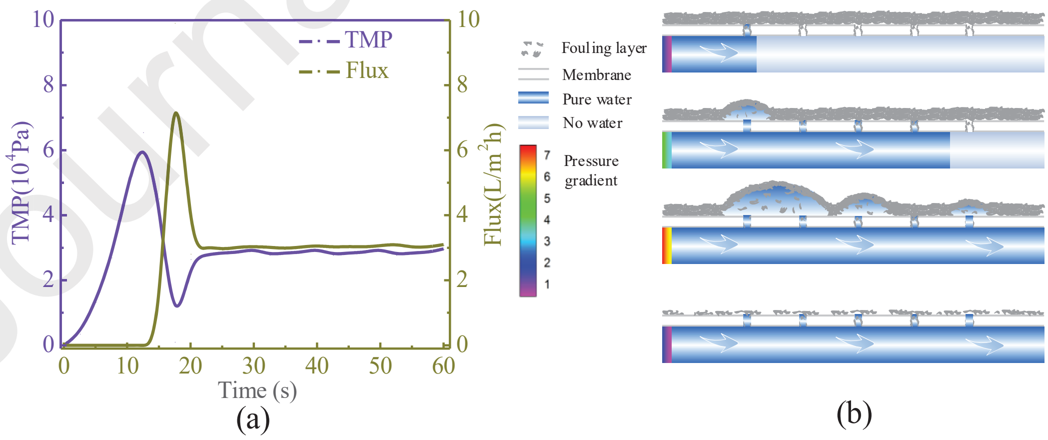

Fig. 2 Hysteresis phenomenon: the out-of-step changes in TMP and flux

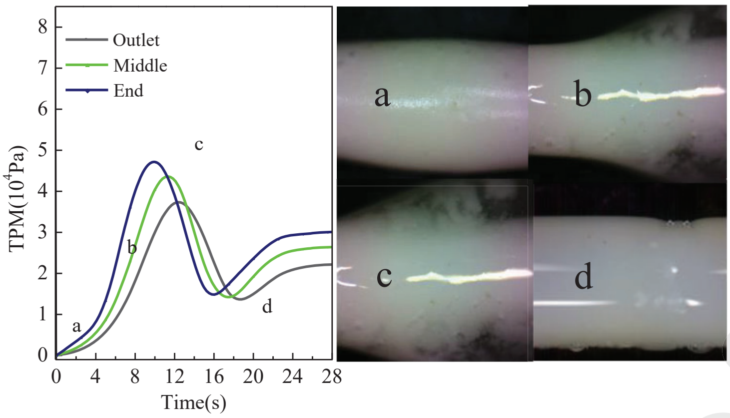

Fig. 3 Hysteresis phenomenon of fouled membrane backwashing with flow of 85L/h: TMP variation and digital photos

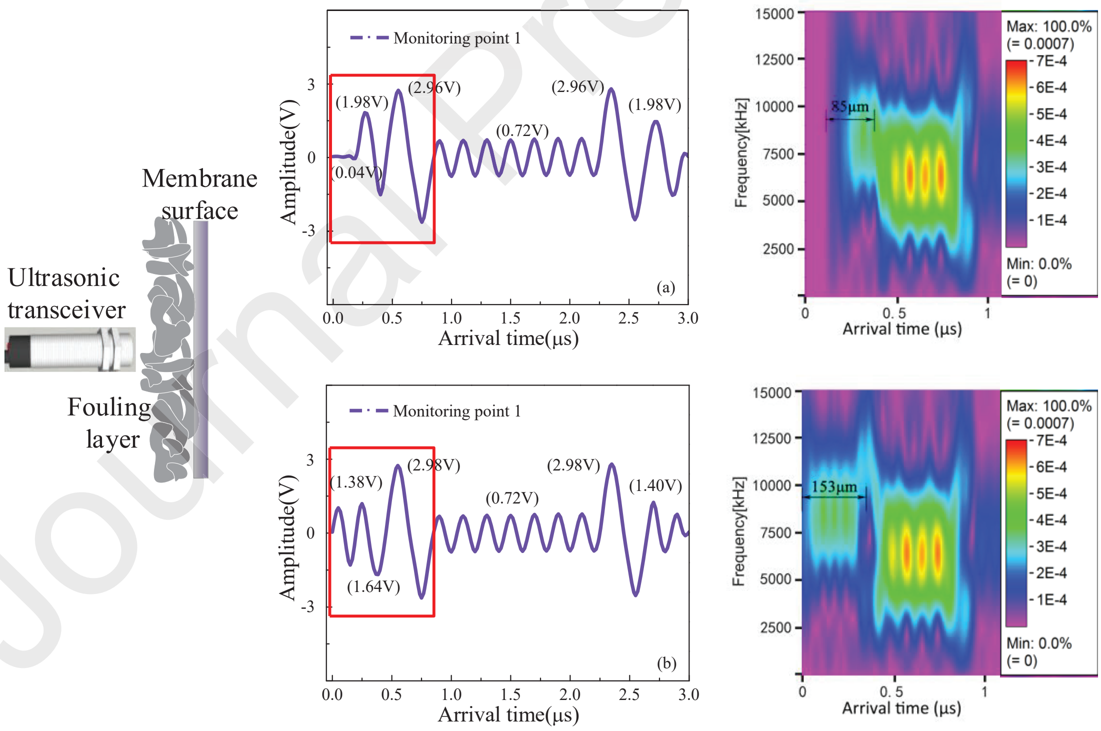

Fig. 4 Ultrasonic signals and 2D contour diagram of the hysteresis phenomenon with 0.6 m membrane under backwashing flow of 85L/h: (a) Ultrasonic signal of fouled membrane (b) Ultrasonic signal at the beginning of backwashing (hysteresis phenomenon)

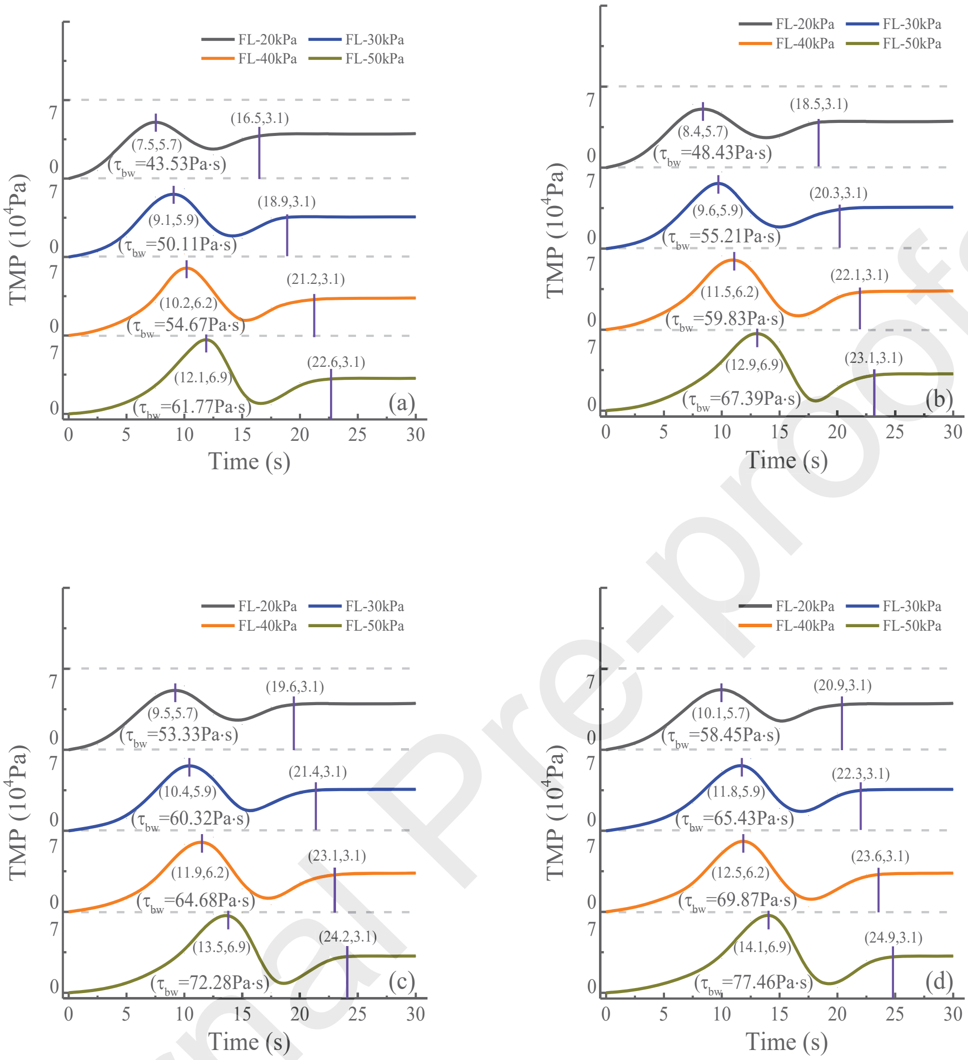

Fig. 5 TMP variation of different fouling levels under backwashing flow of 85L/h: (a) 0.6 m; (b) 0.9 m; (c) 1.2 m; (d) 1.5 m

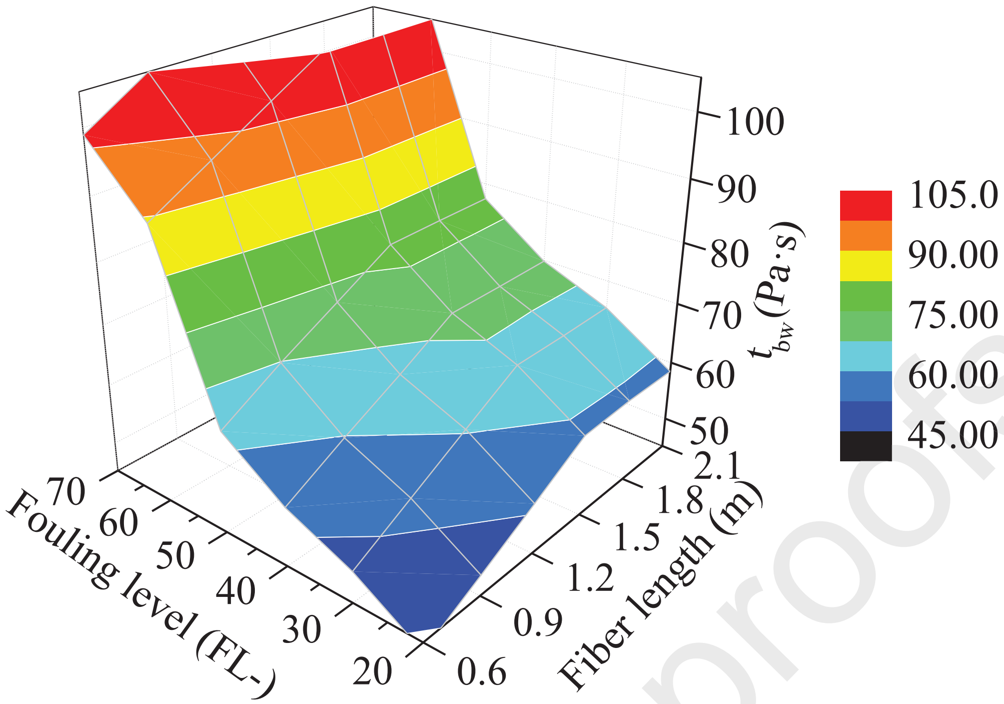

Fig. 6 Relationship between fouling level, fiber length vs "τ_{bw}"

Graphical abstract

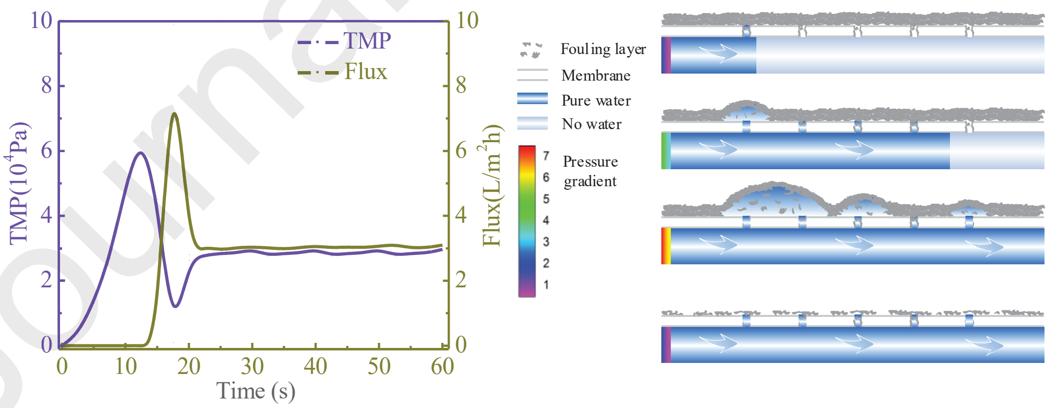

Highlights